Geophysical Research Letters

RESEARCH LETTER
10.1029/2021GL096197

Zonal Structure of Tropical Pacific Surface Salinity Anomalies Affects ENSO Intensity and Asymmetry

Cong Guan[1,2,3], Feng Tian[1,2,3], Michael J. McPhaden[4], Fan Wang[1,2,3], Shijian Hu[1,2,3], and Rong-Hua Zhang[1,2,3]

[1]Key Laboratory of Ocean Circulation and Waves, Institute of Oceanology, Chinese Academy of Sciences, Qingdao, China, [2]Center for Ocean Mega-Science, Chinese Academy of Sciences, Qingdao, China, [3]Qingdao National Laboratory for Marine Science and Technology, Qingdao, China, [4]NOAA/Pacific Marine Environmental Laboratory, Seattle, WA, USA

Abstract Previous studies have revealed the potential importance of salinity in El Niño-Southern Oscillation (ENSO) asymmetry, but the responsible mechanisms remain unclear. Here, we investigate how the zonal structure of surface salinity anomalies affects ENSO intensity and asymmetry by modifying freshwater flux in ocean general circulation model simulations. Results show that the amplitudes of El Niño and La Niña are both highly sensitive to zonal patterns of salinity anomalies, with the strongest sea surface temperature change occurring when maximum salinity anomalies are located near 170°W. Furthermore, the effect of salinity anomalies in the central Pacific on El Niño warming is larger than those in the western Pacific on La Niña cooling. Thus, the asymmetric salinity anomalies strengthen the temperature asymmetry between El Niño and La Niña. Temperature budget analysis shows that vertical mixing and entrainment due to salinity-induced changes in stratification are a major response to different zonal patterns of freshwater flux forcing.

Plain Language Summary Salinity has been suggested to play active roles in the development of ENSO events by affecting vertical stratification. Recent studies found that maximum salinity anomalies are located in the central equatorial Pacific (CEP) during El Niño and in the western equatorial Pacific (WEP) during La Niña. This pattern suggests a role for salinity in ENSO temperature asymmetry, but the underlying mechanisms are unclear. In this study, we conduct a series of sensitivity experiments to investigate salinity effects on ENSO intensity and asymmetry using an ocean general circulation model. Results show that intensities of both El Niño and La Niña are highly sensitive to the zonal patterns of salinity anomalies in the tropical Pacific. Salinity anomalies have the largest impacts on the development of ENSO events when they are located in the CEP near 170°W. Therefore, salinity anomalies in the CEP contribute to stronger warming during El Niño while those in the WEP lead to relatively weaker cooling during La Niña, which strengthens the sea surface temperature asymmetry between El Niño and La Niña. Our experimental results further show that changes in vertical mixing and entrainment are a major factor in the temperature response to salinity anomalies.

Cong Guan and Feng Tian contributed equally to this work.

Key Points:

- El Niño-Southern Oscillation (ENSO) intensity is sensitive to the zonal location of sea surface salinity (SSS) anomalies and becomes strongest when they are located in the central Pacific
- Asymmetric zonal structure of SSS anomalies strengthens the asymmetry of sea surface temperature (SST) anomalies between El Niño and La Niña
- Vertical mixing and entrainment dominate SSS-related SST changes during ENSO cycle

Supporting Information:

Supporting Information may be found in the online version of this article.

Correspondence to:

F. Wang,
fwang@qdio.ac.cn

Citation:

Guan, C., Tian, F., McPhaden, M. J., Wang, F., Hu, S., & Zhang, R.-H. (2022). Zonal structure of tropical Pacific surface salinity anomalies affects ENSO intensity and asymmetry. *Geophysical Research Letters*, *49*, e2021GL096197. https://doi.org/10.1029/2021GL096197

Received 29 SEP 2021
Accepted 20 DEC 2021

Author Contributions:

Conceptualization: Cong Guan, Fan Wang
Data curation: Cong Guan, Feng Tian
Formal analysis: Cong Guan, Feng Tian
Funding acquisition: Cong Guan, Fan Wang
Investigation: Cong Guan, Feng Tian

1. Introduction

Understanding the complexity of El Niño-Southern Oscillation (ENSO) has been a long-standing issue and key to improving forecast model skill on seasonal-to-interannual timescales (Guan & McPhaden, 2016; McPhaden et al., 2006; Timmermann et al., 2018). Understanding the amplitude and spatial asymmetry in sea surface temperature (SST) between warm phase (El Niño) and cold phase (La Niña), is particularly challenging. This asymmetry, with larger SST anomalies during El Niño than during La Niña, is manifest by a positive SST skewness in the eastern Pacific and a negative skewness in the western Pacific (An et al., 2021; Burgers & Stephenson, 1999; Dommenget et al., 2013). A large number of previous studies have focused on role of air-sea coupling processes in modulating ENSO asymmetry (An & Jin, 2004; Choi et al., 2013; Guan, McPhaden et al., 2019; Levine & Jin, 2010; Su et al., 2010). Freshwater flux (FWF) and resultant sea surface salinity (SSS) exhibit large interannual variability in the equatorial Pacific (e.g., Schneider, 2004), but how these processes affect the ENSO asymmetry is largely unexplored.

In the western-central tropical Pacific, the FWF forcing and salinity act as a positive feedback effect on SST variability associated with ENSO (Maes et al., 2006; Vialard et al., 2002; Zhang & Busalacchi, 2009; Zheng & Zhang, 2012). During El Niño, large positive FWF and negative SSS anomalies enhance the vertical stratification in the upper ocean. A thicker barrier layer appears between the mixed layer and isothermal layer, which warms the

Methodology: Feng Tian, Rong-Hua Zhang
Supervision: Michael J. McPhaden, Fan Wang
Writing – original draft: Cong Guan
Writing – review & editing: Feng Tian, Michael J. McPhaden, Shijian Hu

upper layer by reducing the subsurface entrainment of cold water and vertical mixing (Ando & McPhaden, 1997; Bosc et al., 2009; Maes et al., 2002, 2006; Vialard & Delecluse, 1998a, 1998b). Based on coupled model analysis, Zhang et al. (2012) found the FWF effects can enhance cooling during La Niña and warming during El Niño respectively, through changes in salinity and buoyancy flux that modulating the vertical mixing and entrainment in the upper ocean. Gao et al. (2020) further diagnosed that the FWF effects on ENSO SST are mainly though salinity changes. However, these studies are mainly focused on FWF and salinity effects over the entire ENSO cycle, with less attention paid to the differences between El Niño and La Niña. Additionally, modeling studies suggested that adequately representing salinity processes in ocean models can improve the simulations of ENSO variability (e.g., Maes et al., 2005; Zhang, 2015; Zhang et al., 2010; Zhao et al., 2014).

Recent increases in salinity observations have made it possible to investigate the role of salinity in ENSO asymmetry (Qu et al., 2014). For example, based on 17-year Argo observational data set, Guan, Hu, et al. (2019, hereafter G2019) found maximum salinity anomalies appear in the central equatorial Pacific during El Niño, while they are located further west in the western equatorial Pacific during La Niña. They suggested that different zonal locations of salinity anomalies may have an impact on ENSO temperature asymmetry through affecting vertical density stratification. However, whether the asymmetric SST anomaly pattern during the ENSO cycle is sensitive to the zonal pattern of salinity anomalies and how precisely salinity affects ENSO asymmetry remains unclear. In this study, we will address these questions through a series of numerical experiments using an ocean general circulation model (OGCM).

The remainder of the paper is outlined as follows. We will describe the model configuration and experimental design in Section 2. In Section 3, we will diagnose the sensitivity of ENSO intensity to the zonal patterns of salinity anomalies. The impacts of salinity on ENSO temperature asymmetry will be examined in Section 4, followed by a summary and discussion in Section 5.

2. Model and Experimental Design

The OGCM adopted here is a primitive equation and reduced gravity model with a vertical sigma (σ) coordinate (Gent & Cane, 1989), covering the entire tropical Pacific basin. The model has 20 vertical layers with varying σ values and a mixed layer at the top determined by a mixed layer model (Chen et al., 1994). FWF (precipitation minus evaporation) is treated as a natural boundary condition to represent complete hydrology (Murtugudde & Busalacchi, 1998; Zhang et al., 2010). Other aspects of model configuration are described in the supplementary material. SST is from Extended Reconstructed Sea Surface Temperature Version 5 (Huang et al., 2017). Precipitation and evaporation are from the Global Precipitation Climatology Project (Adler et al., 2003) and the Objectively Analyzed Air-Sea Heat Fluxes (Yu & Weller, 2007), respectively. Wind stress is obtained from NCEP/NCAR reanalysis (Kalnay et al., 1996). All these data are monthly from January 1979 to December 2016. This OGCM is well suited for simulating dynamical variabilities in the equatorial Pacific and has been widely used to investigate effects of FWF and surface salinity on ENSO (e.g., Luo et al., 2005; Murtugudde et al., 1996; Zhang & Busalacchi, 2009; Zhang et al., 2010, 2018).

To diagnose the salinity effects on ENSO SST, we simulate salinity anomalies by changing the strength and patterns of FWF forcing. FWF affects the ocean through modulating the upper-layer salinity and the mixed layer depth due to buoyancy fluxes. These fluxes have a direct and immediate impact on SSS on interannual time scales (Gao et al., 2020). Therefore, for simplicity we will interpret FWF effects in terms of salinity responses in this study.

Sensitivity experiments are executed in 2-year composite El Niño and La Niña (detailed designs can be found in the Supporting Information S1 and Table S1). ENSO composites of wind stress are constructed to drive the ocean model for two years. Spatial features of ENSO SST anomalies are well represented in the OGCM forced only by these wind fields (left panel in Figure 1). In particular, maximum El Niño SST anomalies are located within 160°W–105°W, which is more to the east than the maximum La Niña anomalies within 170°E−120°W. These differences lead to positive SST skewness east of the dateline and negative skewness in the west, which is generally consistent with previous results (e.g., Burgers & Stephenson, 1999; Dommenget et al., 2013).

An FWF strength test is first conducted by adding α times (α = 1, 2, 3) the observed 2-year composite FWF anomalies during El Niño and La Niña (Figure S1). To reproduce SSS anomalies that are close to the observations

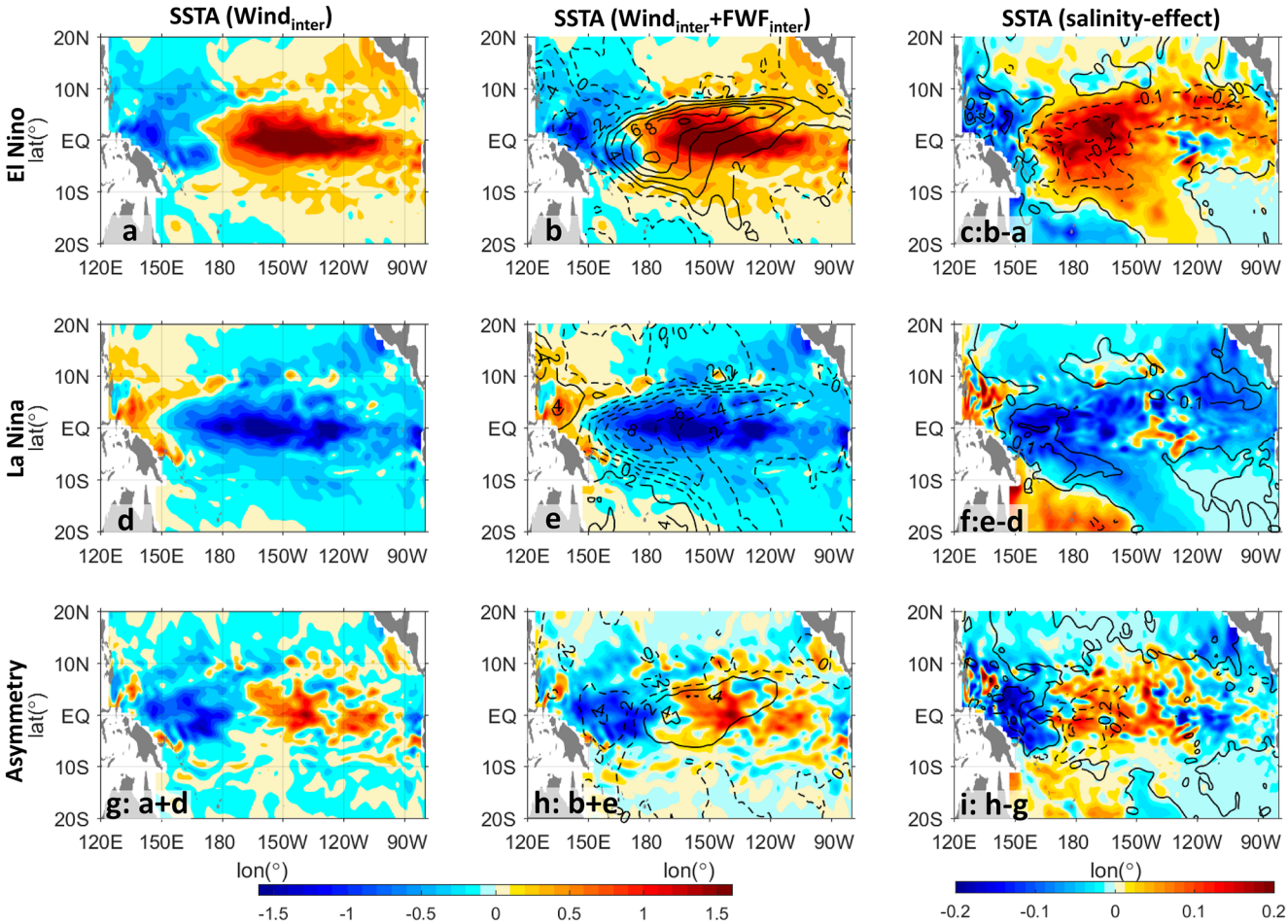

Figure 1. Sea surface temperature (SST) anomalies (shaded) during the mature phase (December–February) of El Niño (a–c), La Niña (d–f) and their differences (g–i) in the tropical Pacific. SST anomalies forced only by the interannual wind stress anomalies are shown in the left panel, SST anomalies forced by both interannual wind stress and twice observed freshwater flux (FWF) anomalies (in contour lines) are shown in the middle, and SST anomalies with sea surface salinity (SSS) anomalies (in contour lines) overlaid induced by the FWF effects (left minus middle) are shown in the right. The unit for SST is °C, for FWF mm/day and for SSS psu.

during the ENSO events (e.g., as Figure 1 in G2019) and also highlight role of salinity effects, we choose twice FWF strength ($\alpha = 2$, as shown in Figures 1b and 1e) as a reference in the following experiments. During both El Niño and La Niña, FWF anomalies start in July with 3 mm/day, gradually increase to maximum exceeding 9 mm/day in winter and weaken in spring (Figures S6a and S6c). During the mature phases, it is shown that maximum FWF anomalies appear in the central equatorial Pacific (CEP; defined here as 170°E−150°W, 5°S–5°N) during El Niño and in the western equatorial Pacific (WEP; 120°E−170°E, 5°S–5°N) during La Niña (Figures S1a and S1b). Under these FWF forcing scenarios, SSS anomalies during El Niño appear in the CEP with maxima exceeding 0.2 psu (Figures 1c and S1d), leading to an enhanced surface warming of 0.2°C (Figure 1c). During La Niña, SSS anomalies occur in the WEP with maxima more than 0.1 psu (Figures 1f and S1g), accompanied by extra cooling up to −0.2°C. As for the asymmetric features between El Niño and La Niña (Figure 1i), SSS anomalies present a dipole structure as seen from Argo analyses in G2019. More importantly, the salinity-induced SST anomalies also exhibit a dipole pattern in the western-central Pacific within 10°S–10°N, with a negative pole west of the dateline and a positive pole in the central Pacific. These results preliminarily reveal that FWF and salinity can enhance the intensity and asymmetry of ENSO SST, which will be further unfolded in the next sections.

We aware that prescribing FWF in OGCM does not allow for ocean feedbacks to the atmosphere as occurs in a coupled system. For example, FWF can lead to an SST response that modifies atmospheric convection and surface wind convergence to promote the Bjerknes feedback. However, our focus in this study is on how FWF-forced salinity variations affect SST via oceanic processes in a forced ocean model framework. This approach provides

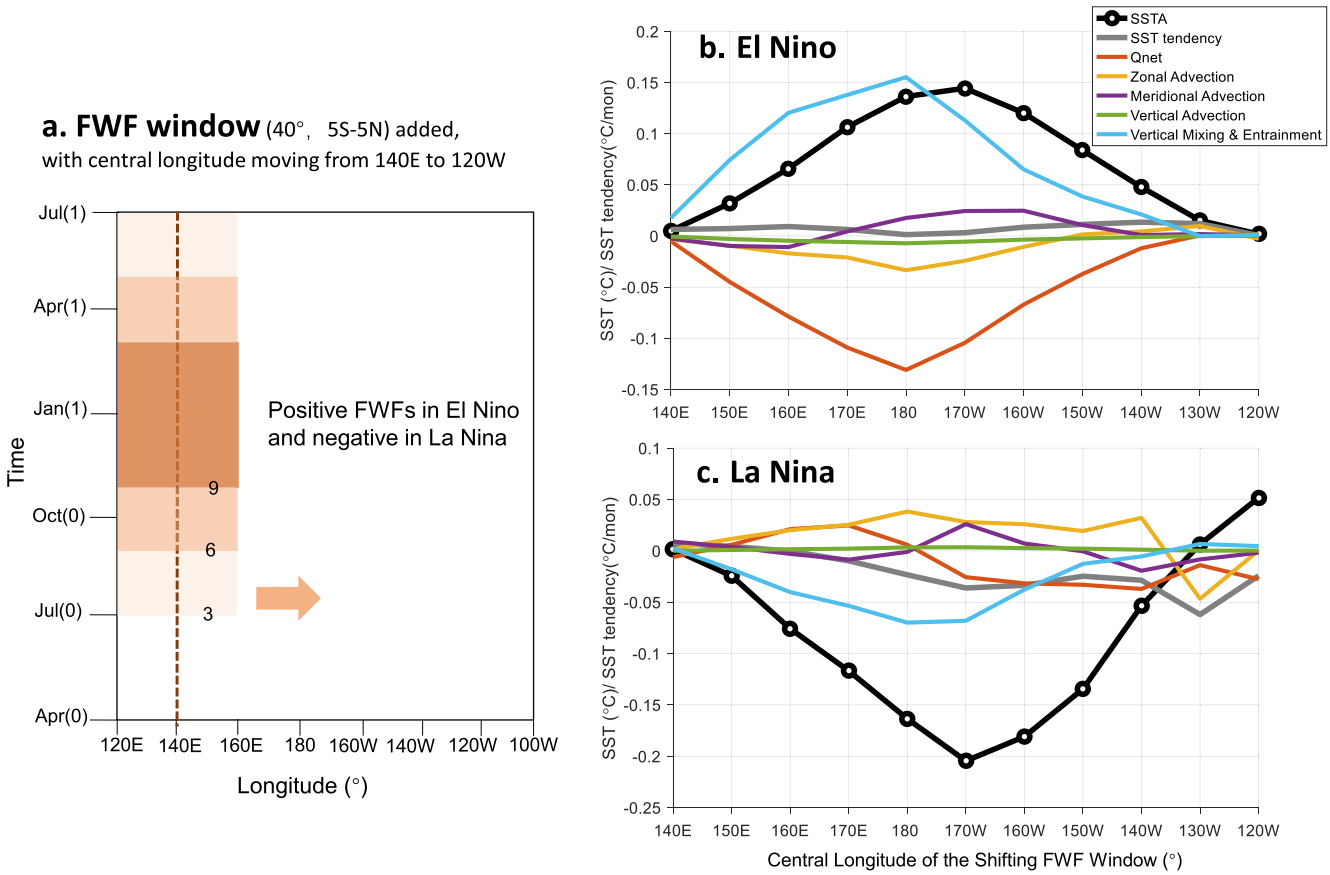

Figure 2. The freshwater flux (FWF) sliding window (a) and their forced sea surface temperature (SST) anomalies (thick black lines) during the mature phases and temperature budget terms (color lines) during the developing phases of El Niño (b) and La Niña (c) averaged in the Niño4 region. The X-coordinates of (b) and (c) are the central longitudes of the FWF forcing window in each experiment.

indications for SST tendencies in response to atmospheric forcing as opposed to simulating the equilibrium response of the coupled air-sea system. We note though these FWF-induced SST anomalies in the OGCM can be greatly amplified in air-sea coupled models (Gao et al., 2020; Zhang et al., 2019). We also note that though the barrier layer cannot be accurately simulated due to the vertical coordinate structure of the model, FWF changes the static stability across the base of the mixed layer and modify the rate at which entrainment and vertical mixing bring cold water up from the thermocline. Thus, the model mimics the effects of barrier layers in response to FWF without actually simulating them.

3. The Sensitivity of ENSO SST Intensity to SSS Anomaly Longitude

The sensitivity of ENSO SST intensity to the longitude of SSS anomalies is diagnosed by adding an ideal pattern of FWF anomalies in the equatorial Pacific from July (0) to July (1) in the 2-year simulations (Figure 2a). The FWF window is set to span 40° in longitude within 5°S–5°N. According to magnitudes and evolutions of the twice FWF composites (Figures S6a and S6c), the FWF intensity in El Niño is increased gradually from July, September to November of the first year as 3, 6–9 mm/day, then decreased symmetrically from March, May to July of the next year. The FWF intensity during La Niña has the same evolution but with negative magnitudes. Then we shift the window progressively eastward by 10° with a central longitude from 140°E to 120°W, superimposed on the mean climatological FWF field in the OGCM, to perform 11 groups of sensitivity experiments during El Niño and La Niña, respectively. Thus, the differences between the sensitivity experiments and the control experiments forced by climatological FWF field indicate the effects of zonal variations in FWF and how they influence salinity anomalies and the evolution of ENSO.

With anomalous FWF forcing, the western-central equatorial Pacific becomes immediately fresher during El Niño and saltier during La Niña (Figures S2–S5). The SSS anomalies are found to have similar amplitudes and shift eastward along with the FWF window in either El Niño or La Niña event. In response to the FWF forcing and its effects on salinity, SST anomalies, however, exhibit a different evolution depending on the zonal location of FWF and SSS anomalies, with its strongest responses in the CEP. Salinity-induced SST anomalies averaged in the Niño4 region (160°E−150°W, 5°S–5°N) during the mature phases of El Niño and La Niña, are shown in Figures 2b and 2c, respectively. It is found that the SST anomalies in the El Niño experiments are all positive and present a clear "V"-type distribution, with the strongest SST anomalies of 0.15°C when the FWF window is centered at the 170°W in the CEP. During the La Niña group, the SST anomalies in the Niño4 region present a similar distribution that are strongest (−0.20°C) at 170°W and become gradually weaker to the west and east, even turning to positive anomalies east of 130°W. Therefore, we conclude that both El Niño and La Niña are very sensitive to the zonal locations of salinity anomalies; salinity effects on SST are the strongest when salinity anomalies are centered near 170°W in the CEP.

To examine what processes in the model control SST changes in response to SSS anomalies, mixed layer heat budgets in the Niño4 region are analyzed during the ENSO developing phases (defined as August [0]-November [0]). Results (Figures 2b and 2c) show that during El Niño, SST tendencies are positive in all the experiments, indicating salinity anomalies in all the locations can produce warming effects on the development phase of El Niño. Among the budget terms, the change in vertical mixing and entrainment is prominently positive with its peak of more than 0.15°C month^{-1} near the dateline, which is largely dampened by the negative surface net heat flux. Meridional advection is weakly positive, and zonal advection is weak negative in the central Pacific, whereas vertical advection is very small. During La Niña, the SST tendency is generally negative in response to salinity anomalies at all locations, becoming stronger to the east. The change in vertical mixing and entrainment is negative and contributes most in the western-central Pacific. The surface net heat flux is weakly positive in the western Pacific and tends to be negative east to the dateline. Zonal advection tends to be the largest positive term. In summary, for both El Niño and La Niña, the dominant oceanic process that results in the SST response to the zonal location of SSS anomalies is vertical mixing and entrainment, which contribute most remarkably in the CEP to the development of ENSO SST anomalies. Why are effects of FWF and salinity most pronounced in the CEP? Zheng et al. (2014) found that salinity controls near surface density stratification in the CEP, in contrast to the temperature-dominant controls in near surface density stratification in the western Pacific on the interannual time scale. Therefore, compared to other parts of equatorial Pacific, salinity anomalies in the CEP will be most effective on the stratification stability, and hence the ENSO SST.

4. Salinity Effects on ENSO SST Asymmetry

As discussed in Section 3, SSS anomalies in the central Pacific can result in stronger SST anomalies during both El Niño and La Niña than those in the western Pacific. Thus, another important question is does this difference in the zonal location of maximum salinity anomalies affect the El Niño-La Niña SST asymmetry?

Note that the composite FWF anomalies generally are found in the central Pacific with a maximum centered at 170°W on the equator during El Niño but in the western Pacific with maximum centered around 165°E on the equator during La Niña (Figure 1). For the sake of discussion, the two scenarios are identified as the CEP case and WEP case, respectively. We further use these two cases to perform a group of sensitivity experiments to explore the relative effects of salinity anomalies in the central Pacific or western Pacific on ENSO asymmetry. Sensitivity experiments are designed separately through superimposing the FWF climatology with positive CEP FWF or negative WEP FWF during El Niño, and negative CEP FWF or positive WEP FWF during La Niña (Figure S6). The control experiment is solely forced by the FWF climatology.

Figure 3 shows the evolution of SSS and SST anomalies in response to the CEP and WEP FWF forcing, respectively. During El Niño, positive SSS anomalies are generated in the CEP and negative anomalies in the west from June (0) in both cases (Figures 3a and 3b). Affected by the positive salinity anomalies, clear warming occurs in the central Pacific and subsequently reaches its peak in the El Niño mature phase. It is noted that the maximum positive SST anomalies are found more eastward by up to 10° longitudes in the CEP case than in the WEP case, resulting in a clear dipole structure as indicated by a difference (Figure 3c). In addition, the CEP-case SST anomalies also have larger amplitudes, indicating that the CEP location of salinity anomalies favors stronger El

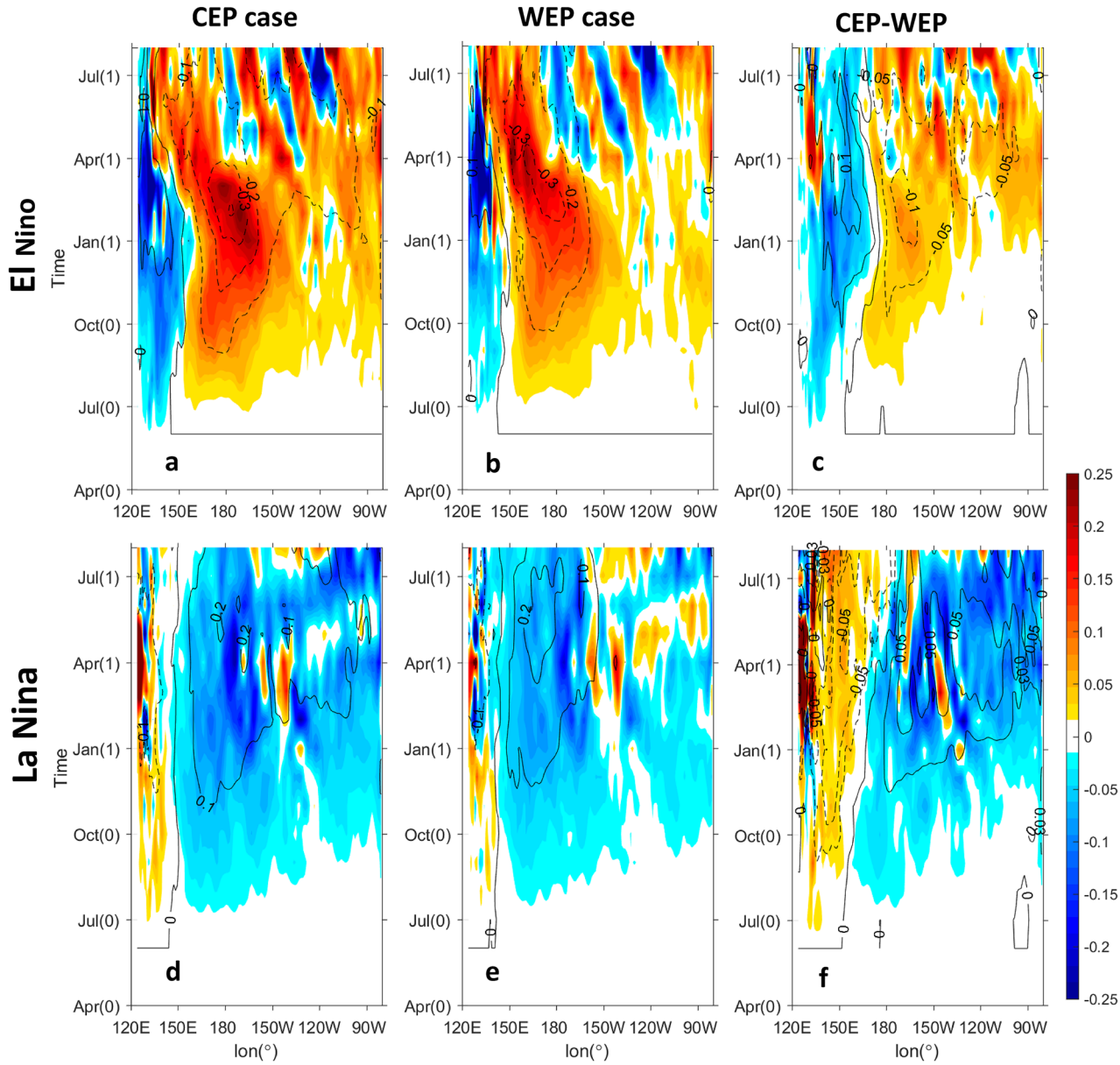

Figure 3. Sea surface salinity (SSS) anomalies (lines) and sea surface temperature (SST) anomalies (shaded) during El Niño (a, b) and La Niña (c, d) in the equatorial Pacific forced by the two types of freshwater flux (FWF) cases.

Niño warming. During La Niña, most of the surface equatorial Pacific becomes saltier due to the negative FWF anomalies except for the far western Pacific, resulting in cooling broadly along the equatorial Pacific and warming in the far west in both cases. Compared to the WEP mode, the CEP-case SST anomalies appear slightly more eastward with a stronger amplitude, especially in the La Niña mature phase, leading to a dipole structure in the differences (Figure 3f).

To make comparisons quantitatively, SST anomalies averaged between 5°S and 5°N during the mature phases of El Niño and La Niña are depicted in Figures 4a and 4b. It shows that the larger ENSO SST anomalies emerge in the central Pacific in CEP-case experiments than in the WEP case. Compared to the asymmetry driven only by the wind forcing (Figure 1g), the CEP FWF increases the El Niño warming in the Niño4 region by 26%, larger than the WEP case of 20%. During La Niña, the CEP FWF increases SST cooling in Niño4 by 17%, which is larger than the 13% extra cooling by the WEP FWF. Therefore, CEP FWF and salinity favor stronger ENSO events than those in the WEP cases, consistent with our results in Section 3. Based on a mixed layer temperature budget

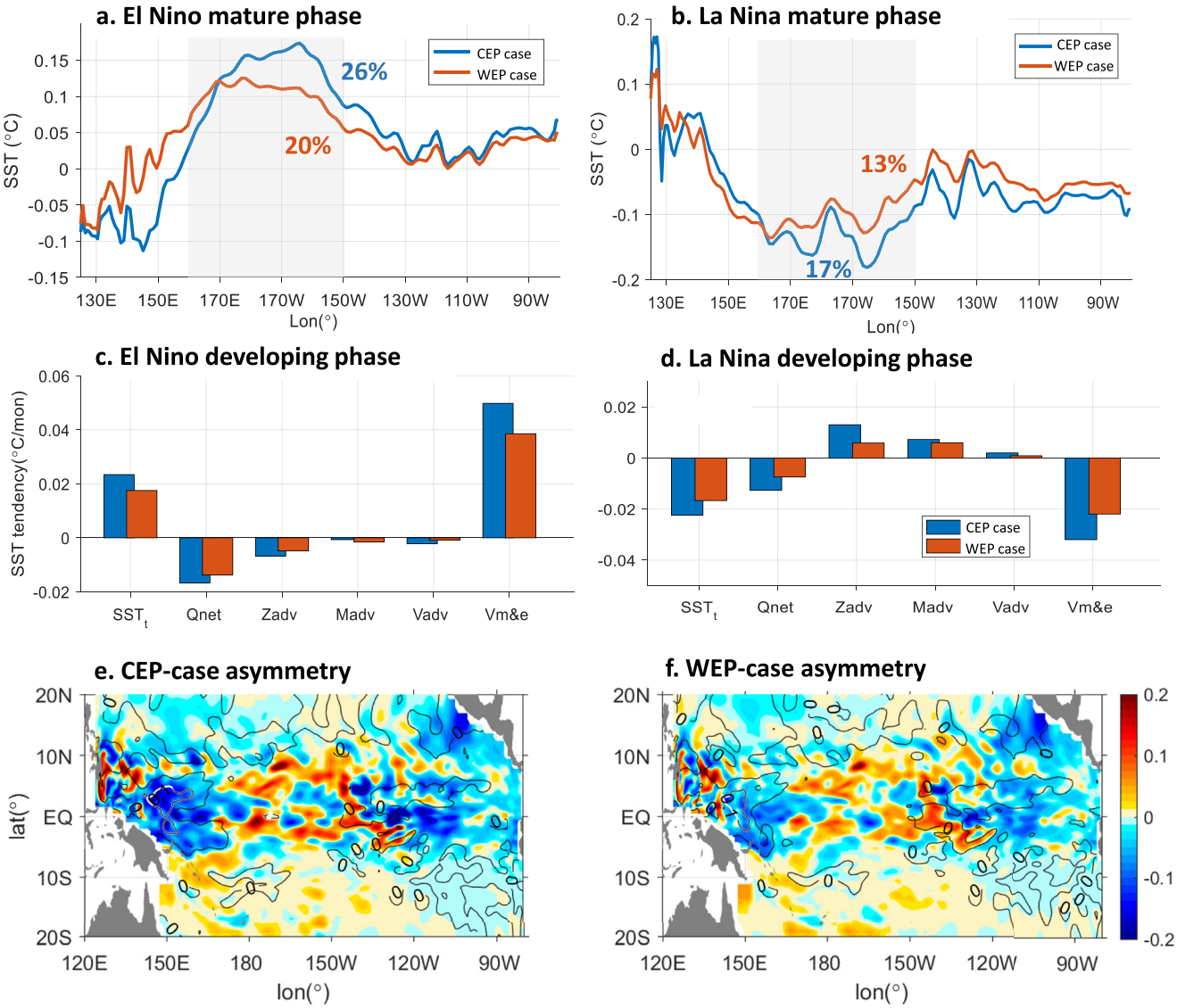

Figure 4. Sea surface temperature (SST) anomalies forced by the central equatorial Pacific (CEP) and WEP freshwater flux (FWF) cases during the mature phases of El Niño and La Niña in the equatorial Pacific (5°S–5°N) are shown in (a) and (b). Temperature budget terms averaged in the Niño 4 region during the developing phases of El Niño and La Niña are shown in (c) and (d), respectively. Asymmetric sea surface salinity (SSS) anomalies (lines) and SST anomalies (shaded) between El Niño and La Niña are shown in **e** for the CEP and (f) for the WEP FWF experiments.

analysis in ENSO developing phases, we find that the SST tendencies in the CEP case are clearly stronger than those in the WEP case for both events. Intensified vertical mixing and entrainment process accounts for the greater SST anomalies in the CEP case during El Niño, while both vertical mixing and entrainment and net surface heat flux contribute to the stronger SST anomalies during La Niña.

Note that in reality, negative salinity anomalies appear as in CEP case during El Niño (Figure 1c), while positive anomalies appear as in WEP during La Niña (Figure 1f), with their difference resulting in a dipole structure of SST anomalies in the western-central Pacific (Figure 1i). However, if there are no difference in the zonal locations of salinity anomalies between El Niño and La Niña, assuming both are under CEP or WEP FWF conditions, the asymmetry in SST anomalies induced by the salinity effects is largely weakened as shown in Figures 4e and 4f, especially under the WEP case. Therefore, the results show that FWF and salinity effects play active roles in ENSO SST asymmetry, and the different zonal patterns of salinity anomalies between El Niño and La Niña strengthen the asymmetry in ENSO SST.

5. Summary and Discussion

This study examined the effects of FWF and sea surface salinity on ENSO intensity and asymmetry based on a series of OGCM experiments. We find that both the El Niño and La Niña SST anomalies are highly sensitive to the zonal patterns of freshwater flux and salinity, and these salinity effects are the strongest when maximum salinity anomalies occur near 170°W in the central Pacific, leading to an extra warming of 0.15°C during El Niño and cooling of −0.20°C during La Niña in the central Pacific.

Salinity effects on the ENSO asymmetry are further examined by a series of sensitivity experiments forced by CEP and WEP FWF forcing. Results show that CEP FWF leads to the central Pacific warming during El Niño while WEP FWF increases La Niña cooling in the western Pacific. The difference between the two cases leads to positive SST skewness in the central Pacific and negative skewness in the western Pacific, which clearly enhances the ENSO SST asymmetry. By alternatively applying these two FWF cases to El Niño and La Niña experiments, it is found that the CEP FWF drives stronger SST amplitudes in both El Niño and La Niña than the WEP case. The asymmetric feature of ENSO SST is clearly weakened if El Niño and La Niña are under the same FWF case. Therefore, we conclude that the CEP FWF leads to a stronger warming during El Niño, while the WEP FWF have weaker effects on La Niña cooling. Hence, the different zonal patterns of FWF and salinity anomalies between El Niño and La Niña directly lead to strengthening of the SST asymmetry in ENSO.

The dynamical mechanisms that determine the SST changes in response to different zonal patterns of FWF and salinity are further diagnosed based on temperature budget analysis. Results show that effects of FWF and salinity anomalies on SST are basically though vertical mixing and entrainment from below the base of mixed layer. As shown in Zheng et al. (2014), salinity controls upper-layer density stratification in the CEP in contrast to the temperature-dominant stratification in the WEP. So that when salinity anomalies occur in the CEP during ENSO events, the vertical mixing and entrainment of subsurface cold water becomes more effective, as a result of stratification changes than those in the WEP. Schematic diagram for these mechanisms can be found in Figure S7 in the Supporting Information S1. As for why the FWF and salinity anomalies have such different zonal patterns between El Niño and La Niña, these asymmetric FWF patterns are simply controlled by the zonal movement of ENSO-associated precipitation, while the asymmetry in SSS anomalies is basically dominated by the nonlinear zonal advection (G2019). Though these features are originally responses to ENSO SST variations, they in turn strengthen the SST asymmetry though differential salinity effects.

We note that because we use only one model in this study, there may be some effect of model biases on our results due to model configuration (e.g., grid resolution, vertical mixing scheme, vertical coordinate structure, etc.). Multi-model intercomparisons from Phase 6 of the Coupled Model Intercomparison Project (CMIP6)/ Flux-Anomaly-Forced Model Intercomparison Project (FAFMIP) may provide some insights into this issue in the future. It is also interesting to find that SST anomalies are stronger during La Niña than El Niño in response to the FWF window centered at 170°W, probably induced by the difference in net surface heat flux (Figures 2b and 2c) based on our methodology. Further examination of this feature however is beyond of the scope of this study. In the meantime, this study will help inform our understanding of mechanisms of ENSO SST asymmetry and improve simulation skills of ENSO complexity in climate models, from the perspective of salinity effect.

Data Availability Statement

Open Research: NCEP/NCAR reanalysis data are from IRI/LDEO Climate Data Library (http://iridl.ldeo.columbia.edu/SOURCES/.NOAA/.NCEP-NCAR/.CDAS-1/.DAILY/.Diagnostic/.surface/.taux/); GPCP monthly precipitation data and monthly evaporation data in OA Flux are from Asia-Pacific Data- Research Center (APDRC; http://apdrc.soest.hawaii.edu/data/data.php). NOAA_ERSST_V5 data are provided by the NOAA/OAR/ESRL PSD from Web site at https://psl.noaa.gov/data/gridded/data.noaa.ersst.v5.html. Model output data related to this study are available on the figshare data archive, https://doi.org/10.6084/m9.figshare.16635064.v2.

Acknowledgments
The authors thank the two anonymous reviewers for their constructive comments on the original version of this manuscript. This work was supported by the National Natural Science Foundation of China (Grants 41730534, 42176008, and 41806016). S. Hu was supported by the National Natural Science Foundation of China (Grants 41776018 and 91858101). F. Tian was supported by the Strategic Priority Research Program of the Chinese Academy of Sciences (Grant No. XDB42000000) and the National Natural Science Foundation of China (Grants 42006001). R.-H. Zhang was supported by the National Natural Science Foundation of China (Grants 42030410). PMEL contribution no. 5296.

References

Adler, R. F., Huffman, G. J., Chang, A., Ferraro, R., Xie, P.-P., Janowiak, J., et al. (2003). The version-2 global precipitation climatology project (GPCP) monthly precipitation analysis (1979-present). *Journal of Hydrometeorology*, *4*, 1147–1167. https://doi.org/10.1175/1525-7541(2003)004<1147:TVGPCP>2.0.CO;2

An, S.-I., & Jin, F.-F. (2004). Nonlinearity and asymmetry of ENSO. *Journal of Climate*, *17*, 2399–2412. https://doi.org/10.1175/1520-0442(2004)017<2399:naaoe>2.0.co;2

An, S.-I., Tziperman, E., Okumura, Y. M., & Li, T. (2021). ENSO irregularity and asymmetry. In M. J. McPhaden, A. Santoso, W. Cai (Eds.), *El Niño southern oscillation in a changing climate*. *AGU monograph* (pp. 153–172). https://doi.org/10.1002/9781119548164.ch7

Ando, K., & McPhaden, M. J. (1997). Variability of surface layer hydrography in the tropical Pacific Ocean. *Journal of Geophysical Research*, *102*(C10), 23063–23078. https://doi.org/10.1029/97jc01443

Bosc, C., Delcroix, T., & Maes, C. (2009). Barrier layer variability in the western Pacific warm pool from 2000 to 2007. *Journal of Geophysical Research*, *114*, C06023. https://doi.org/10.1029/2008jc005187

Burgers, G., & Stephenson, D. B. (1999). The "normality" of El Niño. *Geophysical Research Letters*, *26*, 1027–1030. https://doi.org/10.1029/1999gl900161

Chen, D., Rothstein, L. M., & Busalacchi, A. J. (1994). A hybrid vertical mixing scheme and its application to tropical ocean models. *Journal of Physical Oceanography*, *24*, 2156–2179. https://doi.org/10.1175/1520-0485(1994)024<2156:ahvmsa>2.0.co;2

Choi, K. Y., Vecchi, G. A., & Wittenberg, A. T. (2013). ENSO transition, duration, and amplitude asymmetries: Role of the nonlinear wind stress coupling in a conceptual model. *Journal of Climate*, *26*, 9462–9476. https://doi.org/10.1175/jcli-d-13-00045.1

Dommenget, D., Bayr, T., & Frauen, C. (2013). Analysis of the non-linearity in the pattern and time evolution of El Niño southern oscillation. *Climate Dynamics*, *40*, 2825–2847. https://doi.org/10.1007/s00382-012-1475-0

Gao, C., Zhang, R.-H., Karnauskas, K. B., Zhang, L., & Tian, F. (2020). Separating freshwater flux effects on ENSO in a hybrid coupled model of the tropical Pacific. *Climate Dynamics*, *54*(11), 4605–4626. https://doi.org/10.1007/s00382-020-05245-y

Gent, P. R., & Cane, M. A. (1989). A reduced gravity, primitive equation model of the upper equatorial ocean. *Journal of Computational Physics*, *81*, 444–480. https://doi.org/10.1016/0021-9991(89)90216-7

Guan, C., Hu, S., McPhaden, M. J., Wang, F., Gao, S., & Hou, Y. (2019). Dipole structure of mixed layer salinity in response to El Niño-La Niña asymmetry in the tropical pacific. *Geophysical Research Letters*, *46*(21), 12165–12172. https://doi.org/10.1029/2019gl084817

Guan, C., & McPhaden, M. J. (2016). Ocean processes affecting the twenty-first-century shift in ENSO SST variability. *Journal of Climate*, *29*, 6861–6879. https://doi.org/10.1175/jcli-d-15-0870.1

Guan, C., McPhaden, M. J., Wang, F., & Hu, S. (2019). Quantifying the role of oceanic feedbacks on ENSO asymmetry. *Geophysical Research Letters*, *46*, 2140–2148. https://doi.org/10.1029/2018gl081332

Huang, B., Thorne, P. W., Banzon, V. F., Boyer, T., Chepurin, G., Lawrimore, J. H., et al. (2017). Extended reconstructed Sea surface temperature, Version 5 (ERSSTv5): Upgrades, validations, and intercomparisons. *Journal of Climate*, *30*, 8179–8205. https://doi.org/10.1175/JCLI-D-16-0836.1

Kalnay, E., Kanamitsu, M., Kistler, R., Collins, W., Deaven, D., Gandin, L., et al. (1996). The NCEP/NCAR 40-year reanalysis project. *Bulletin of the American Meteorological Society*, *77*, 437–471. https://doi.org/10.1175/1520-0477(1996)077<0437:tnyrp>2.0.co;2

Levine, A. F. Z., & Jin, F. F. (2010). Noise-induced instability in the ENSO recharge oscillator. *Journal of the Atmospheric Sciences*, *67*, 529–542. https://doi.org/10.1175/2009jas3213.1

Luo, Y., Rothstein, L. M., Zhang, R.-H., & Busalacchi, A. J. (2005). On the connection between South Pacific subtropical spiciness anomalies and decadal equatorial variability in an ocean general circulation model. *Journal of Geophysical Research*, *110*, C10002. https://doi.org/10.1029/2004jc002655

Maes, C., Ando, K., Delcroix, T., Kessler, W. S., McPhaden, M. J., & Roemmich, D. (2006). Observed correlation of surface salinity, temperature and barrier layer at the eastern edge of the western Pacific warm pool. *Geophysical Research Letters*, *33*, L06601. https://doi.org/10.1029/2005gl024772

Maes, C., Picaut, J., & Belamari, S. (2002). Salinity barrier layer and onset of El Niño in a Pacific coupled model. *Geophysical Research Letters*, *29*(24), 5951–5954. https://doi.org/10.1029/2002gl016029

Maes, C., Picaut, J., & Belamari, S. (2005). Importance of the salinity barrier layer for the buildup of El Niño. *Journal of Climate*, *18*(1). https://doi.org/10.1175/jcli-3214.1

McPhaden, M. J., Zebiak, S. E., & Glantz, M. H. (2006). ENSO as an integrating concept in Earth science. *Science*, *314*, 1740–1745. https://doi.org/10.1126/science.1132588

Murtugudde, R., & Busalacchi, A. J. (1998). Salinity effects in a tropical ocean model. *Journal of geophysical Research*, *103*, 3283–3300. https://doi.org/10.1029/97jc02438

Murtugudde, R., Seager, R., & Busalacchi, A. (1996). Simulation of the tropical oceans with an ocean GCM coupled to an atmospheric mixed-layer model. *Journal of Climate*, *9*, 1795–1815. https://doi.org/10.1175/1520-0442(1996)009<1795:sottow>2.0.co;2

Qu, T., Song, Y. T., & Maes, C. (2014). Sea surface salinity and barrier layer variability in the equatorial Pacific as seen from Aquarius and Argo. *Journal of Geophysical Research: Oceans*, *119*, 15–29. https://doi.org/10.1002/2013jc009375

Schneider, N. (2004). The response of tropical climate to the equatorial emergence of spiciness anomalies. *Journal of Climate*, *17*(5), 1083–1095. https://doi.org/10.1175/1520-0442(2004)017<1083:trotct>2.0.co;2

Su, J., Zhang, R., Li, T., Rong, X.-S., Kug, J., & Hong, C. C. (2010). Causes of the El Niño & La Niña amplitude asymmetry in the equatorial eastern Pacific. *Journal of Climate*, *23*, 605–617. https://doi.org/10.1175/2009jcli2894.1

Timmermann, A., An, S., Kug, J. S., Jin, F. F., Cai, W., Capotondi, A., et al. (2018). El Niño? Southern oscillation complexity. *Nature*, *559*, 535–545. https://doi.org/10.1038/s41586-018-0252-6

Vialard, J., & Delecluse, P. (1998a). An OGCM study for the TOGA decade. Part I: Role of salinity in the physics of the western Pacific fresh pool. *Journal of Physical Oceanography*, *28*, 1071–1088. https://doi.org/10.1175/1520-0485(1998)028<1071:aosftt>2.0.co;2

Vialard, J., & Delecluse, P. (1998b). An OGCM study for the TOGA decade. Part II: Barrier-layer formation and variability. *Journal of Physical Oceanography*, *28*, 1089–1106. https://doi.org/10.1175/1520-0485(1998)028<1089:aosftt>2.0.co;2

Vialard, J., Delecluse, P., & Menkes, C. (2002). A modeling study of salinity variability and its effects in the tropical Pacific Ocean during the 1993–1999 period. *Journal of Geophysical Research*, *107*(C12), 1–14. https://doi.org/10.1029/2000jc000758

Yu, L., & Weller, R. A. (2007). Objectively analyzed Air–Sea heat fluxes for the global ice-free oceans (1981–2005). *Bulletin of the American Meteorological Society*, *88*, 527–540. https://doi.org/10.1175/BAMS-88-4-527

Zhang, R.-H. (2015). A hybrid coupled model for the Pacific Ocean–atmosphere system. Part I: Description and basic performance. *Advances in Atmospheric Sciences*, *32*(3), 301–318. https://doi.org/10.1007/s00376-014-3266-5

Zhang, R.-H., & Busalacchi, A. J. (2009). Freshwater flux (FWF)-induced oceanic feedback in a hybrid coupled model of the tropical Pacific. *Journal of Climate*, *22*, 853–879. https://doi.org/10.1175/2008jcli2543.1

Zhang, R.-H., Tian, F., Busalacchi, A. J., & Wang, X. (2019). Freshwater flux and ocean chlorophyll produce nonlinear feedbacks in the tropical pacific. *Journal of Climate*, *32*(7), 2037–2055. https://doi.org/10.1175/jcli-d-18-0430.1

Zhang, R.-H., Tian, F., & Wang, X. (2018). Ocean chlorophyll-induced heating feedbacks on ENSO in a coupled ocean physics-biology model forced by prescribed wind anomalies. *Journal of Climate*, *31*, 1811–1832. https://doi.org/10.1175/jcli-d-17-0505.1

Zhang, R.-H., Wang, G., Chen, D., Busalacchi, A. J., & Hackert,E. C. (2010). Interannual biases induced by freshwater flux and coupled feedback in the tropical Pacific. *Monthly Weather Review*, *138*(5), 1715–1737. https://doi.org/10.1175/2009mwr3054.1

Zhang, R.-H., Zheng, F., Zhu, J. S., Pei, Y. H., Zheng, Q. N., & Wang, Z. G. (2012). Modulation of El Niño-southern oscillation by freshwater flux and salinity variability in the tropical Pacific. *Advances in Atmospheric Sciences*, *29*, 647–660. https://doi.org/10.1007/s00376-012-1235-4

Zhao, M., Hendon, H. H., Alves, O., & Yin, Y. (2014). Impact of improved assimilation of temperature and salinity for coupled model seasonal forecasts. *Climate Dynamics*, *42*, 2565–2583. https://doi.org/10.1007/s00382-014-2081-0

Zheng, F., & Zhang, R.-H. (2012). Effects of interannual salinity variability and freshwater flux forcing on the development of the 2007/08 La Niña event diagnosed from Argo and satellite data. *Dynamics of Atmospheres and Oceans*, *57*, 45–57. https://doi.org/10.1016/j.dynatmoce.2012.06.002

Zheng, F., Zhang, R.-H., & Zhu, J. (2014). Effects of interannual salinity variability on the barrier layer in the western-central equatorial Pacific: A diagnostic analysis from Argo. *Advances in Atmospheric Sciences*, *31*, 532–542. https://doi.org/10.1007/s00376-013-3061-8

Reference From the Supporting Information

Seager, R., Blumenthal, M. B., & Kushnir, Y. (1995). An advective atmospheric mixed layer model for ocean modeling purposes: Global simulation of surface heat fluxes. *Journal of Climate*, *8*, 1951–1964. https://doi.org/10.1175/1520-0442(1995)008<1951:aaamlm>2.0.co;2